

## Chapter 7

---

# HSPA Radio Access Network Design

---

Jamil Yusuf Khan and Xinzhi Yan

### Contents

7.1	Introduction .....	234
7.2	UTRAN Architecture .....	237
7.2.1	UTRAN Functionalities .....	238
7.2.2	UTRAN Interface Functionalities .....	239
7.2.2.1	$I_u$ Interface .....	239
7.2.2.2	$I_{ur}$ Interface .....	240
7.2.2.3	$I_{ub}$ Interface .....	241
7.2.3	Radio Resource Management .....	241
7.2.3.1	Combining/Splitting .....	241
7.2.3.2	Connection Setup and Release .....	242
7.2.4	Radio Bearer Allocation .....	242
7.2.5	Radio Protocol Functions .....	243
7.3	UTRAN Protocol Structure .....	243
7.3.1	HSDPA Protocol Structure .....	244
7.3.2	HSUPA Protocol Structure .....	246
7.3.3	UTRAN MAC Protocol .....	248
7.4	E-UTRAN Architecture .....	251
7.5	UTRAN Design: $I_{ub}$ Link Resource Management Algorithms .....	252
7.5.1	Joint $I_{ub}$ Link Flow Control Model .....	254
7.6	Air Interface and $I_{ub}$ Parameter Interdependencies .....	259
7.6.1	Simulation Model .....	259
7.6.2	Performance Analysis .....	260

- 7.6.3 Adaptive  $I_{ub}$  Link Management Algorithm ..... 265
  - 7.6.3.1 Estimating HSDPA Air Interface Average Throughput ..... 265
  - 7.6.3.2 Adaptive  $I_{ub}$  Bandwidth Allocation ..... 266
- 7.7 Summary ..... 268
- References ..... 269

**7.1 Introduction**

Radio access network (RAN) is one of the key elements of a mobile communication network. The RAN plays a key role in offering multimedia services to users as well as maintaining QoS (quality of service) for different services. The design of RAN parameters is very important in maintaining the appropriate QoS for different services, particularly in a packet-switched wireless network where resource-sharing techniques are applied to maximize network resource utilization and to minimize operating costs. The UMTS (Universal Mobile Telecommunications System) network uses a standard mobile telephone network architecture where various functionalities are grouped and distributed over logical subnetworks that are connected through different logical interfaces. Functionally, all UMTS network elements are grouped within the RAN known as UTRAN (UMTS Terrestrial Radio Access Network) and the core network (CN), which connects the UTRAN to external networks such as PSTNs (public switched telephone networks) and the Internet. Figure 7.1 shows the generic UMTS architecture, depicting the basic reference points and interfaces [1]. The separation of subnetworks allows ease of interconnection and independence of signaling and data transparent networks. Currently, both the legacy WCDMA (Wideband Code Division Multiple Access) network and the HSPA (High-Speed Packet Access) network share the same CN but have different UTRAN architectures, functions, and resource management algorithms. UMTS networks, which are currently offering both legacy and HSDPA (High-Speed Downlink Packet Access)/HSPA services, have upgraded their UTRAN functionalities based on Release 5/6 or higher 3GPP (3rd Generation Partnership Project) standards. The new standard supports both legacy services as well as advanced packet based HSPA services. Introduction of HSDPA and HSUPA (High-Speed Uplink Packet Access) services have increased the packet-switched traffic volume in the UTRAN and in the CN. The UTRAN architecture is currently evolving toward a high data rate and high QoS network. Recently, the E-UTRAN (Evolved UTRAN) architecture was introduced; it was designed to support advanced packet-switched services using a flat network architecture to accommodate new services as well as to offer high QoS to all services.

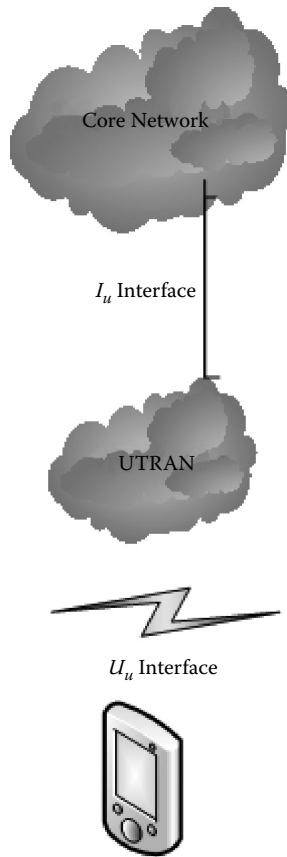


**Figure 7.1** UMTS architecture.

The UTRAN consists of two main network elements that form the radio network subsystem (RNS). Those elements are Node-B, which is the base station, and the RNC (radio network controller), the key network controller. The user equipment (UE) connects to the UTRAN using the  $U_u$  interface (radio link) as shown in Figure 7.1. Elements of the UE consist of a mobile equipment (ME), which is a radio terminal, and the UMTS subscriber identity module (USIM). The UTRAN architecture of the HSPA network is defined by 3GPP Release 6 and onward standards, which are quite different from the legacy Release 99 standard. The HSDPA standard was introduced in Release 5 of the 3GPP standard in 2002, followed by the introduction of the HSUPA standard in Release 6 in 2004. The HSUPA and HSDPA standards are unified, and the combined standard is known as the HSPA standard. Since the introduction of the HSPA standard, the role of the UTRAN has changed significantly due to the support of diverse types of

packet-switched traffic. The HSPA standard was developed mainly to support high data rate packet-switched traffic with low latency and high QoS requirements. With the introduction of the E-UTRAN architecture, the expected target transmission packet delay on the UE to RNC link in an HSPA network should be maintained at less than 10 ms [2]. To support the low latency and high QoS (packet loss, jitter, etc.) requirements, the UTRAN architecture is gradually evolving by incorporating various advanced functionalities. In Release 7 of the 3GPP standard, several HSPA enhancements were introduced, to include providing major improvements to end-user QoS performance, support of high data rate services, inclusion of specialized services such as VoIP (Voice over Internet Protocol), and increasing network efficiency [3]. To further enhance the QoS of HSPA services, the 3GPP is also proposing a new flat architecture similar to the LTE (Long Term Evolution) architecture introduced in Release 8 [4]. Improvements in the QoS and latency of HSPA connections can be achieved by developing enhanced resource management algorithms for the UTRAN; these are beyond the scope of 3GPP standards and have been left for researchers to develop.

To achieve high QoS and low latency for HSPA connections it will be necessary to develop efficient radio resource management algorithms for various interfaces and network entities of the UTRAN. The 3GPP standards do not specify any specific algorithms; rather, it is left to vendors to develop appropriate algorithms that offer high QoS for different services. This chapter concentrates on the development and performance analysis of radio resource management algorithms for the  $I_{ub}$  interface, which is one of the key interfaces of the UTRAN. The QoS profile of the  $I_{ub}$  link can significantly influence both the uplink and downlink as well as control traffic. Before presenting the resource management algorithms, various key elements of the UTRAN are introduced in this chapter. The chapter is organized into sections as follows:

- “UTRAN Architecture” overviews the UTRAN network and interface architectures. This section also reviews the functional requirements of the UTRAN.
- “UTRAN Protocol Structure” describes several key functional procedures and protocol architecture of the UTRAN.
- “E-UTRAN Architecture” briefly introduces the Evolved UTRAN architecture and lists some of the initial specifications.
- “UTRAN Design:  $I_{ub}$  Link Resource Management Algorithms” reviews different UTRAN resource management algorithms, mainly concentrating on the  $I_{ub}$  interface, which is responsible for connecting the Node-B and the RNC. This section also very briefly reviews some algorithms developed by different researchers.

- “Air Interface and  $I_{ub}$  Parameter Interdependencies” examines the HSDPA air interface and the  $I_{ub}$  link parameter interdependencies to evaluate the performance of the joint resource management algorithm.
- The “Summary” provides conclusions.

## 7.2 UTRAN Architecture

The UTRAN consists of a number of RNSs connecting UEs to the CN. Figure 7.2 shows the basic UTRAN architecture with different logical interfaces connecting various elements of the network. In the UTRAN, Node-B is connected to the RNC using the  $I_{ub}$  interface. The  $I_{ub}$  interface allows the RNC and the Node-B to negotiate radio resource usage to support different connections according to the QoS requirements of services supported by these connections. The  $I_{ub}$  link supports three types of information transfer: (1) various user data, (2) signaling related to user data transmission, and (3) logical operations and maintenance data of Node Bs. The  $I_{ur}$  interface is used to connect two RNCs located in different radio network subsystems to exchange data and signaling information. The  $I_{ur}$  interface provides capabilities to support the mobility of UEs between RNSs. The  $I_{ur}$  interface could connect the RNCs over a direct physical connection or through a virtual connection. In the UTRAN, RNCs are connected to the core network using the  $I_u$  interface. All traffic to and from external networks passes through the  $I_u$  interface, which supports three distinct service domains. These domains are packet switched (PS), circuit switched (CS), and broadcast (BC). According to the 3GPP standard, at any time there shall not be more than one  $I_{ur}$ -PS interface toward the PS domain except under certain

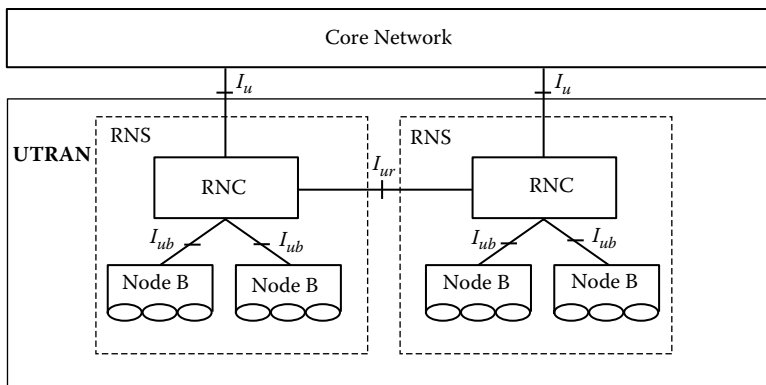


**Figure 7.2** UTRAN architecture showing the different elements of the core network. (3GPP, TS25.401, R8, UTRAN Overall Description, v.8.2.0, Fig. 4, 16, 2008. With permission from ETSI.)

**Table 7.1 Summary of Radio Resource Management Functionalities of the Different Elements of UTRAN**

<i>Node-B</i>	<i>SRNC</i>	<i>DRNC</i>
Packet scheduling Dynamic resource allocation QoS provisioning Load control mechanisms Uplink power control	QoS parameter mapping Handover control Uplink outer-loop Power control (for HSUPA connections)	Admission control Initial uplink power setting Radio resource allocation Code distribution Load control

special network configurations. Similarly, each RNC shall not have more than one  $I_u$ -CS interface toward the core network except in circumstances where inter- or intra-system handovers or the SNRS relocation operation is supported.

An RNC in an RNS may take on multiple networking roles. The RNC could be a *serving* RNC (SRNC) connecting UEs to the CN via the UTRAN using different  $I_u$  interfaces. The SNRC also performs L2 (Layer 2) processing and all basic resource management functionalities, such as radio access bearer (RAB) mapping, handover decision, and outer-loop power control [5]. The RNC can also act as a *controller* RNC (CRNC), which controls its own Node-B in an RNS, and is responsible for load and congestion control on the  $I_{ub}$  link. The CRNC also executes the admission control and code allocations of new connections in its own cell. Another RNC configuration known as the *drift* RNC (DRNC) is responsible for performing micro-diversity combining and splitting, as well as routing data between  $I_{ub}$  and  $I_{ur}$  interfaces without performing any L2 processing of user plane data. For HSDPA and HSUPA networks, the radio resource management functionalities are split between the Node-B and the RNC. The radio resource management functionalities of different elements of the UTRAN are summarized in Table 7.1.

### 7.2.1 UTRAN Functionalities

UTRAN functionalities have been developed based on the following principles. In the UTRAN, the CRNC will own all the radio resources of a cell that can be borrowed by a serving RNC to handle all UE connections in the cell. The SNRC is also responsible for dynamic power control of dedicated channels that are admitted by the corresponding CRNC. For HSUPA connections, fast power control function is coordinated by the Node-B. The resource scheduling task within the UTRAN is performed by various RNCs. Dedicated channels are scheduled by the SRNC, whereas the common

channels are scheduled by the CRNC. However, the packet scheduling task on the  $U_u$  interface remains with the Node-B. Admission control is performed by the DRNC, which allocates new radio access bearers or new radio links to HSPA connections. The admission control algorithms should try to avoid overload situations and make a decision based on interference conditions and resource management criteria. On the UTRAN side, the admission control technique is applied on all  $I_{ub}$  and  $U_u$  interfaces. The UTRAN also introduces congestion control techniques to monitor, detect, and handle situations when a system may be reaching an overload circumstance or may have exceeded the overload condition with existing traffic load. Both the admission and congestion control algorithms could be applied on different interfaces based on local traffic and radio transmission conditions to optimize the performance of various interfaces. It is also possible to use joint admission and congestion control algorithms on multiple interfaces to optimize the overall performance of the UTRAN. An end-to-end HSPA connection can be seen as a multi-hop connection involving a number of interfaces ( $U_u$ ,  $I_{ub}$ ,  $I_{ur}$ , and  $I_u$ ) where a congestion control algorithm could be applied locally or jointly between different interfaces to meet the QoS requirements of the HSPA connections. Admission and congestion control algorithms are not specified by 3GPP standards, and it is left to the vendors to develop efficient algorithms within the UTRAN framework.

The UTRAN architecture for the HSPA network has been enhanced compared to the Release 99 standard by incorporating transport channels and associated functionalities to support these enhanced packet-based services. The HS-DSCH (High-Speed Downlink Shared Channel) was introduced to support the HSDPA traffic and the E-DCH (Enhanced Dedicated Channel) was introduced to support the HSUPA traffic. The HSDPA standard introduces several data rate adaptation and control mechanisms to support the peak data rates and high spectral efficiency, as well as higher QoS for asymmetric data traffic. These functionalities are distributed within UTRAN elements and include RNCs, Node-B, and various interfaces. These functionalities are described in following subsections.

## **7.2.2 UTRAN Interface Functionalities**

### **7.2.2.1 $I_u$ Interface**

The  $I_u$  interface was designed to support the interconnection of RNCs to the CN access points offering services in PS, CS, and BC domains. These interfaces offer independence between protocol layers as well as independence between control and user planes [5]. The  $I_u$  interface was developed as an open and multivendor interface to allow the separate evolution of

O&M (Operations and Management) functionalities. The main capabilities of the interface are that it

- Offers procedures to establish, maintain, and release radio access bearers
- Offers SRNS (serving RNS) relocation, intra- and inter-system handovers
- Supports cell broadcast services
- Offers separation of each UE connection on the protocol level for user-specific signaling management
- Offers location-based services using geographical area identifier or global coordinates with uncertainty parameters
- Offers simultaneous access to multiple core network domains for each UE
- Transfers signaling between the UE and the CN
- Offers simultaneous access to multiple CN domains for a single UE
- Offers mechanism for resource reservation for packet data streams
- Has procedures to support multicasting services using MBMS (Multicast Broadcast Multimedia Services) bearer services

#### 7.2.2.2 $I_{ur}$ Interface

The  $I_{ur}$  interface supports the interconnection of RNCs developed by different manufacturers. It also supports the continuation of services between RNSs via the  $I_u$  interface [6]. The main capabilities of the  $I_{ur}$  interface are

- The interface provides capability to support mobility of UEs between different radio network subsystems. The mobility is offered by supporting handover, radio resource management, MBMS connection management, and synchronization between different RNSs.
- The interface supports different types of data streams such as DCH, RACH (Random Access Channel), HS-DSCH, E-DCH transport frames carrying user data and control information between the SRNC and Node-B, and the DRNC.
- Within the UTRAN, the HSDPA traffic is carried by the HS-DSCH frame. A UE may have multiple HS-DSCH data streams on the  $I_{ur}$  interface. The  $I_{ur}$  interface provides a means for transporting MAC-d (dedicated MAC) PDUs (Protocol Data Units). In addition, the interface provides a means to the SRNC for queue reporting and a means for the DRNC to allocate capacity to the SRNC.
- The HSUPA traffic within the UTRAN is carried by E-DCH data frames. The  $I_{ur}$  interface provides the means for transporting  $I_{ub}/I_{ur}$  E-DCH frames carrying user data between Node-B and the SRNC via the DRNC.



A UE may have multiple E-DCH data streams supporting different applications and traffic sources. In addition to the above functionalities, the interface provides the following additional options:

- A means for the Node-B to indicate the number of HARQ transmissions to the SRNC
- A means to indicate to the SRNC for the purpose of reordering connection frame number and subframe numbers that are added by the Node-B.

### 7.2.2.3 $I_{ub}$ Interface

The interface provides an interconnection between the Node-B and the RNC by separating radio network and transport network functionalities to facilitate the introduction of future transmission technologies [7]. This interface has been developed based on several key principles, as follows:

1. The functional division between the RNC and the Node-B.
2. Neither the physical structure nor any internal protocols of the Node-B shall be visible over the  $I_{ub}$  link, thus helping the introduction of new technologies in the future.

The  $I_{ub}$  interface capabilities are similar to the  $I_{ur}$  interface supporting various data streams. The interface provides the means for transporting HSDPA traffic using HS-DSCH frames between the RNC and the Node-B. Similarly, the interface supports HSUPA traffic between the Node-B and the RNC using the E-DCH frames. Each HS-DSCH data stream on the  $I_{ub}$  link is carried on a single transport bearer. For each HS-DSCH data stream, a transport bearer must be established over the  $I_{ub}$  interface. The  $I_{ub}$  interface also supports features similar to the  $I_{ur}$  interface to support HARQ transmission features.

### 7.2.3 Radio Resource Management

Radio resource management is concerned with the allocation and maintenance of communication resources. In a UTRAN network, resources must be shared between circuit-switched and packet-switched connections for resource optimization. To efficiently allocate radio resources, the UE and UTRAN network entities will survey the radio environment by measuring its own and surrounding cells' SNR (signal-to-noise ratio), BER (bit error rate), power profiles, interference, synchronization status, etc. Based on these measurements, various transmission resources are allocated by the RNCs and the Node-B in the UTRAN. Some of the key radio resource management functionalities of a UTRAN are summarized below.

### *7.2.3.1 Combining/Splitting*

This function controls information streams to receive or transmit the same information through multiple physical channels transmitted or received from a single mobile terminal. Multiple physical channels may receive information from different cells particularly in case of a soft handover. Depending on the physical network configuration the combining/splitting function could be carried out at the SRNC, DRNC, or Node-B level.

### *7.2.3.2 Connection Setup and Release*

This function is responsible for the control of end-to-end connection setup and release. The function also maintains the end-to-end connection by using appropriate algorithms to support call QoS and handover executions. This function is located both in the UE and in the RNC.

## **7.2.4 Radio Bearer Allocation**

This function allocates appropriate physical radio channels to users by matching the QoS of a radio bearer with the connection setup request. During the connection setup, users will specify the QoS of the required connection. The function is located in the CRNC and the SRNC. The  $I_u$  interface provides extensive RAB (radio access bearer) management functionalities that control connections between UEs and the CN. Depending on subscription, service, and requested connection QoS, a particular RAB will be selected from a pool of RABs. The CN controls connection establishment, modification, or release of an RAB by initiating appropriate protocol functionalities. These are CN-initiated and UTRAN-executed functionalities. A RAB release request could be generated by the UTRAN when it fails to keep the RAB established for a UE. The RAB characteristics mapping function is used to map appropriate radio access bearers to the  $U_u$  interface and the  $I_u$  interface transport bearer. When the PS domain traffic is carried by the UTRAN, the RNC will perform the mapping between the radio access bearers and the IP-layer QoS functions.

An HSPA network requires support of priorities to accommodate different types of multimedia traffic. The allocation of a priority level of an RAB is determined by the CN based on subscription information, QoS information, etc. According to the above information, the CN requests the UTRAN to establish or modify RAB parameters with an indicated priority level, preemption capability, and the queuing preferences. Queuing and resource preemption can be carried out by the UTRAN according to the preference set up during the call establishment procedure. The radio resource admission control is carried out by the UTRAN when it receives a request to modify or to establish a radio access bearer from the CN. Based

on the request, the UTRAN analyzes the load situation, and then the admission control module either accepts or rejects the request. If a call request is queued, then the request is handled by the RAB queuing, preemption, and priority functions.

The admission control on the  $I_{ub}$  link is based on uplink interference and downlink power information. The admission control module is located in the CRNC. The Node-B reports uplink interference measurements and downlink power information over the  $I_{ub}$  interface. The CRNC controls the reporting procedures, including the reporting frequency. On the  $I_{ub}$  link traffic on high-speed channels (HS-DSCH and E-DCH) is managed by the Node-B.

### 7.2.5 Radio Protocol Functions

This function provides user data and signaling transfer capabilities across the UMTS radio interface by adapting the QoS of various services according to radio transmission conditions. The QoS of different services will depend on the selection and allocation of radio bearers. The UMTS radio protocol includes the following main functionalities:

- Multiplexing of different services using the allocated connection to a UE
- Multiplexing of UEs on various radio bearers
- Segmentation and assembly of information blocks
- Delivering acknowledged and unacknowledged services according to the allocated radio access bearer

## 7.3 UTRAN Protocol Structure

UTRAN functionalities are layered into the radio network layer (RNL) and the transport network layer (TNL). All UTRAN logical nodes and interfaces between them are defined as a part of the RNL. All UTRAN-related functions are only visible in the RNL. For all UTRAN interfaces, their related transport protocol and functionalities are specified in [1, 8]. The TNL provides services for user plane transport, signaling transport, and specific O&M transport. The TNL represents standard transport technology without any UTRAN-specific changes. The general UTRAN protocol architecture is shown in Figure 7.3. The protocol is structured into three vertical planes implementing all TNL and RNL functionalities. The protocol model supports three standard vertical planes: control, user, and signaling. The control plane is mainly responsible for the UMTS control signaling, which includes implementation of the application protocol of different logical interfaces, and the signaling bearer for transporting the application protocol messages.

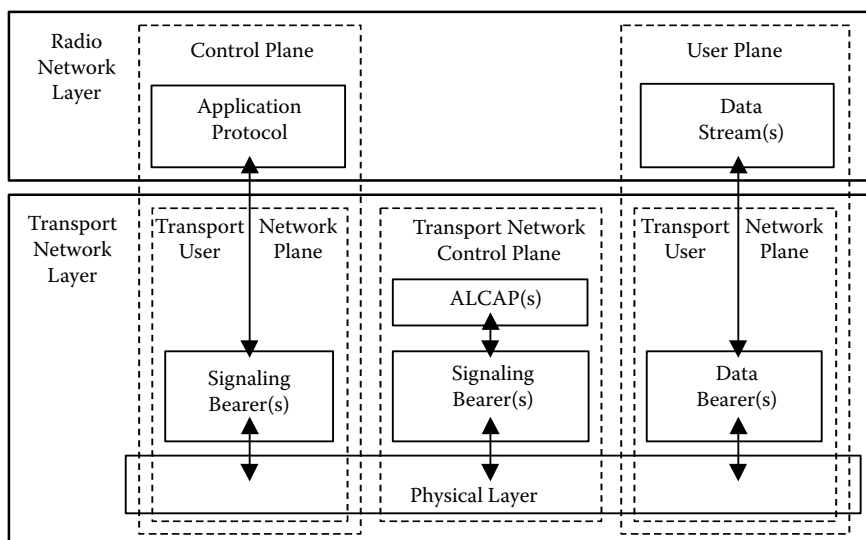


**Figure 7.3 General protocol architecture for UTRAN. (3GPP, TS25.321, R8, Medium Access Control (MAC) Protocol Specification, v.8.4.0, Fig. 10, 39, 2008. With permission from ETSI.)**

One of the main tasks of the application protocol is setting up the bearers of the  $I_{ur}$  interface and then subsequently the radio link for the  $I_{ur}$  and  $I_{ub}$  interfaces. In the three-plane structure, the bearer parameters in the application protocol are not directly tied to the user plane technology. The user plane is responsible for transporting user information, which includes coded voice or voice calls and various types of data streams. The transport network control plane is responsible for control signaling of the transport layer. This layer does not handle any RNL signaling. However, this layer does include the signaling protocol used to set up data bearers and the signaling bearer needed for the ALCAP (Access Link Control Application Part). The ALCAP may not be needed for all types of data bearers. In absence of any ALCAP signaling transaction, transport network control is not required. This situation arises when either preconfigured data bearers or IP-based UTRAN or CN nodes are used. When the transport network control plane is used to set up transport bearers for data traffic in the user plane the following approach is used. First, the control plane establish signaling transactions which is triggered by the set-up of data bearers by the ALCAP protocol specific to the user plane technology. The transport network user plane allocates data bearers in the user plane and signaling bearers for the application protocol. Data bearers in the transport network user plane are directly controlled by the transport network control plane for real-time services.

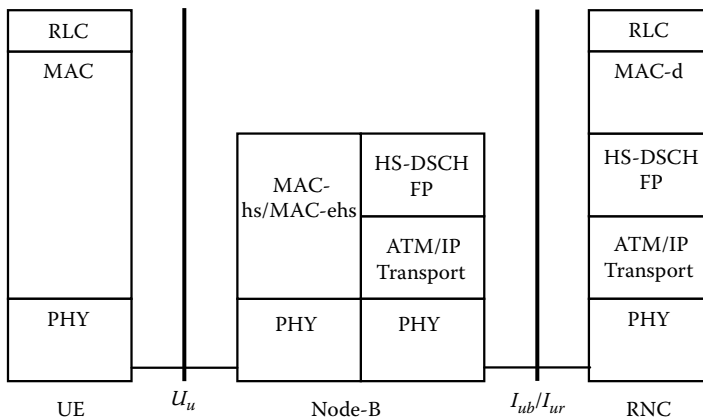


**Figure 7.4** HSDPA protocol architecture.

### 7.3.1 HSDPA Protocol Structure

The UTRAN uses two new transport channels (HS-DSCH and E-DCH) compared to release 99 of 3GPP protocols to support HSDPA and HSUPA traffic flows. The HSDPA user plane protocol architecture is shown in Figure 7.4. The figure shows the distributed nature of the protocol. The Node-B is responsible for scheduling, radio resource allocation, and QoS provisioning and load control mechanisms. The RNC is responsible for QoS parameter mapping, handover control, and maintaining the link to the CN. The HSDPA physical layer at the  $U_u$  interface has been enhanced by incorporating the fast link adaptation procedure by using the adaptive modulation and coding (AMC), and HARQ (Hybrid Automatic Repeat Request) techniques in the Node-B and in the UE. To support the advanced physical layer capabilities, two specialized MAC entities have been introduced, known as MAC-hs (Medium Access Control High Speed) and MAC-ehs (Medium Access Control Enhanced High Speed). The MAC-hs/ehs provide enhanced functionalities such as fast scheduling to facilitate the efficient usage of radio resources to adapt to channel conditions and the network load [8]. To implement HSDPA features, three new channels have been introduced in the physical layer. These channels are HS-DSCH, HS-SCCH (High Speed Shared Common Channel), and the HS-DPCCH (High Speed Dedicated Physical Control Channel). The HS-DSCH carries data in the downlink direction, with the peak rate reaching up to 28.8 Mbps. The HS-SCCH is used to support signaling and the physical layer retransmission procedures. The HS-DPCCH carries various control signals, including the ARQ acknowledgment and the downlink quality feedback information. The HS-DSCH is dynamic in nature, wherein resource sharing can be achieved after

every 2-ms transmission time interval (TTI) utilizing packet schedulers. The physical layer is also responsible for selecting the HS-DSCH parameters such as the transmission data rate based on the terminal capability, number of code allocation, modulation type, and HARQ parameters.

The distributed HSDPA architecture splits the MAC layer between the RNC and the Node-B. MAC PDUs, generated by the RNC and called MAC-d PDUs, are aggregated and sent to the Node-B over the  $I_{ub}$  interface using HS-DSCH frames. The delivery of PDUs over the  $I_{ub}$  interface is managed by a flow control protocol that can act independently for each cmCHPI (Common Transport Channel Priority) used for different UEs. The RLC (radio link control) layer at the RNC is responsible for segmentation and retransmission of user and control data on the downlink. The RNC receives data from the CN, which is appropriately segmented using the RLC protocol. The RLC layer is involved in the data link layer retransmission process when the physical layer retransmission known as HARQ fails or exceeds its retransmission limits. The MAC-d layer is retained in the RNC to handle transport channel switching. The MAC-hs layer is located in the Node-B and is responsible for scheduling, priority handling, HARQ, and selection of an appropriate transport format and resources. The HS-DSCH is the transport channel that carries the user data. The HS-DSCH FP (Frame Protocol) handles the data transport between the RNC and the Node-B. For an HSDPA connection, data received from the CN is encapsulated in a MAC-d PDU and then transmitted over the  $I_{ub}$  link using the HS-DSCH frame. The HS-DSCH FP entity adds header information to form a HS-DSCH FP PDU that is transported to Node-B over a transport bearer. The MAC-hs or MAC-ehs entity in Node-B transfers MAC-hs/ehs PDU to the peer MAC entity in the UE over the  $U_u$  interface. The MAC/L2 protocol at the RNC and at the Node-B could use different types of transport protocols, such as ATM (Asynchronous Transfer Mode) or UDP/IP (User Datagram Protocol/Internet Protocol). The  $I_{ub}$  link requires a flow control mechanism to ensure that Node-B buffers are appropriately utilized and high throughput is obtained on the downlink. The flow control mechanism will be supported by MAC layers at both ends of the  $I_{ub}$  link.

### 7.3.2 HSUPA Protocol Structure

The enhanced uplink was introduced to significantly enhance the capacity of the uplink as well as to improve the QoS (throughput and delay) of uplink traffic [9, 10]. To improve the performance of the uplink it is necessary to enhance the dedicated channels by offering priorities to streaming, interactive, and background services. Appropriate QoS mechanisms must be developed to support packet services such as streaming, interactive, and background data transmission. The enhanced uplink was developed

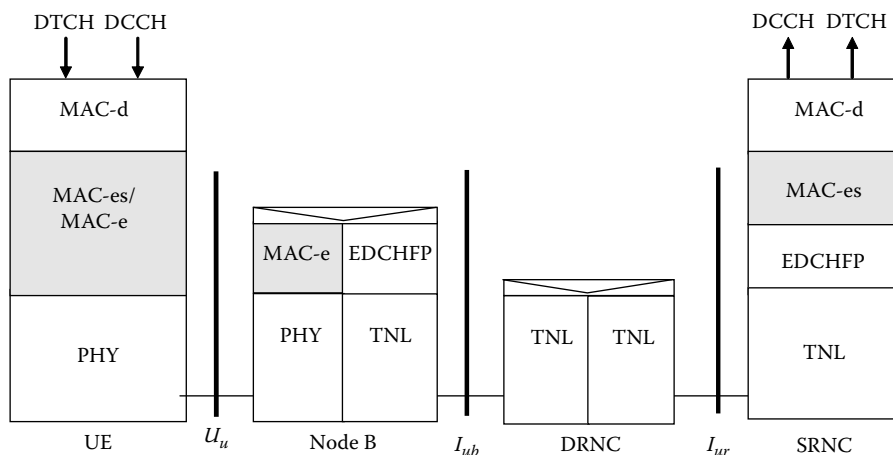


**Figure 7.5** HSUPA protocol stack.

with the view that enhanced terminals can coexist with legacy terminals (specified by Release 99, Release 4, and Release 5). The enhanced uplink was developed to enhance the overall system performance by operating alongside the HSDPA standard. At the same time, it is assumed that the enhanced uplink should operate without any dependency on the deployment of HSDPA features. To support the HSUPA features, the UTRAN protocol introduces new MAC entities: (1) new entities MAC-es/e and MAC-is/i are added in the UE below the MAC-d layer; and (2) new entities MAC-e/MAC-i in the UE handle HARQ retransmissions, scheduling and multiplexing, and the TFC selection tasks. In the Node-B, these entities support HARQ retransmission, scheduling, and demultiplexing operations. In the SRNC, the new entity MAC-es is used to provide in-sequence delivery of PDUs and a data combining function when data is received from multiple Node-Bs to support a soft handover. A reordering function within the MAC-es is used to provide in-sequence delivery of data blocks to the RLC layer. In the CRNC, MAC-e/i entities provide functionalities to support in-sequence delivery of PDUs, disassembly and reassembly of PDUs, and the collision detection function. Figure 7.5 shows the HSUPA protocol architecture, highlighting the new entities in the MAC layer. HSUPA connections use the E-DCH transport channel in the UTRAN to carry user data. The E-DCH MAC entity in the UE transfers the MAC-e/i PDU to its peer MAC entities in the RNC. The E-DCH FP entity adds header information to form the E-DCH FP PDU, which is transported to the RNC over a transport bearer. The PDU generation process is controlled by the interworking function (IWF) at Node-B, which receives data from the UE. The E-DCH channel scheduling is performed by the MAC-e/i entity in the Node-B, and reordering is performed by the

MAC-es/is entity in the RNC. The Node-B performs two types of resource scheduling known as the absolute grant (AG) and the relative grant (RG) [11]. The UE sends a scheduling request to Node-B for permission to transmit; in response to this request, the Node-B sends a grant specifying the data rate of the approved connection. The scheduler uses the E-DCH absolute grant channel (E-AGCH) for transmitting primary or secondary grant (PAG or SAG) information, which caters to large changes in connection data rates. The RG information is sent on the E-DCH relative grant channel (E-RGCH) to send relative grants, which reflect minor changes in the connection data rate. The relative grant allows the Node-B scheduler to incrementally adjust the services grant of the UE under its control. The RG values can take one of three different values: UP, DOWN, or HOLD. The new MAC entity MAC-es/i also performs the task of resource scheduling. This option provides the serving node (Node-B/RNC) a better view of the resource requirements of UE and the amount of resources it can actually use. When any scheduling information is transmitted, its contents must be updated in new transmissions with the buffer status after the application of E-TFC (E-DCH transport format combination).

### 7.3.3 UTRAN MAC Protocol

This section briefly discusses the basics of the UTRAN MAC protocol for the HSDPA and HSUPA standards from a resource management point of view. In the UMTS/HSPA network, the MAC protocol is split between a UE and different entities of the UTRAN. In the MAC layer, the logical channels are mapped on transport channels. The MAC layer is also responsible for selecting the appropriate transport format (TF) for each channel, and this depends on the instantaneous data rate requirements of logical channels. The MAC layer also performs several other important tasks, including priority handling and scheduling of data flow, multiplexing and demultiplexing of PDUs, traffic measurements, and control as specified by the RRC (radio resource controller). [Figure 7.6](#) shows the MAC architecture of the HS-DSCH channel on the UTRAN side. The logical channels are shown on top of the MAC module, whereas the transport channels are shown below the MAC module. In this section the different logical channel characteristics are not discussed; detailed descriptions of these channels can be found in [9, 11]. Newly introduced MAC-hs/MAC-ehs entities handle HS-DSCH channel-specific functions. All data received on HS-DSCH channels are mapped onto MAC-hs/MAC-ehs entities. The MAC-hs/MAC-ehs is configured by the RRC using the MAC control service access point (SAP). The RRC sets the transport format combinations for the HS-DSCH channels. The associated downlink signaling carries information to support the operation of HS-DSCH channels, while the uplink signaling carries feedback information



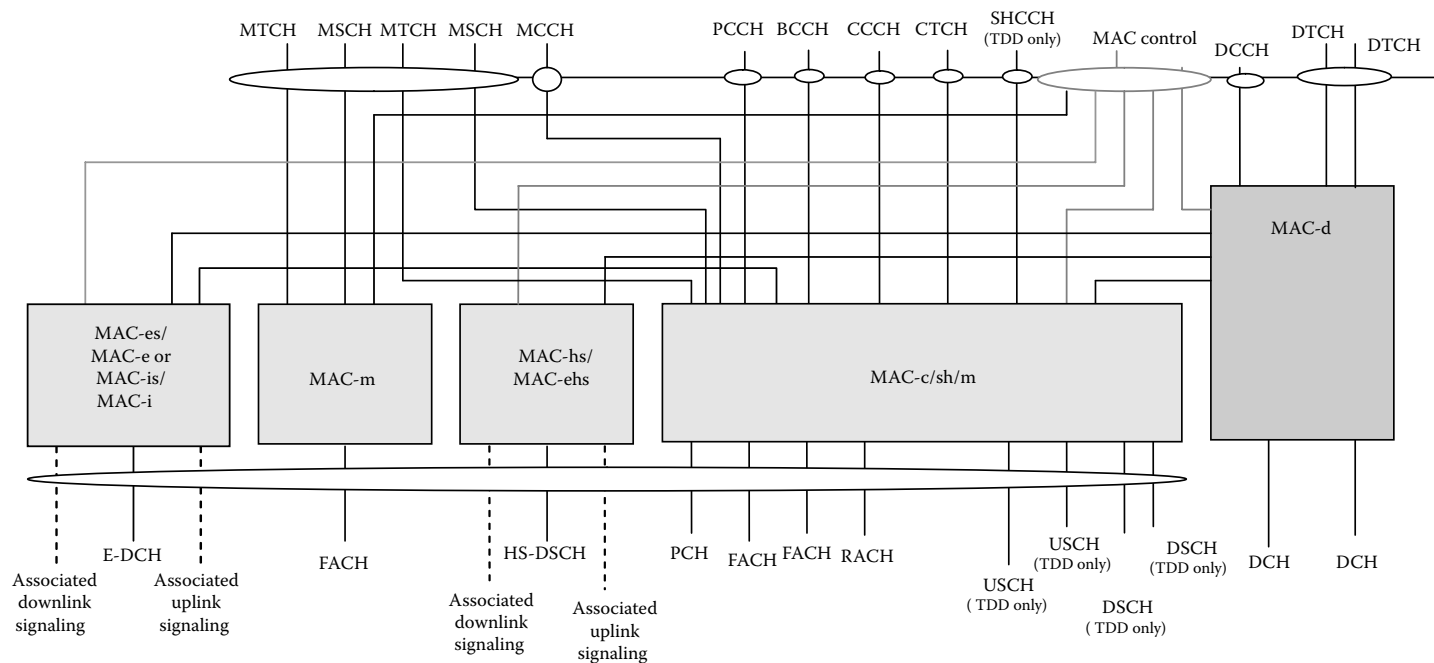


**Figure 7.6** MAC protocol architecture of the HS-DSCH channel. (3GPP, TS25.321, R8, Medium Access Control (MAC) Protocol Specification, v.8.4.0, Fig. 4.2.3.1, 16, 2008. With permission from ETSI.)

such ACK/NACK and CQI (channel quality indicator). On the UTRAN side, one MAC-hs entity is used for each cell to support HS-DSCH data transmission. The MAC-hs is configured by upper layers and is responsible for handling data transmission on the HS-DSCH channel. This entity is also responsible for the management of HSDPA physical resources. The MAC-hs handles the priority of MAC-d PDUs and performs the following two resource management functions:

- *Flow control.* This is a companion flow control function of the MAC-c/sh/m entity. These functions jointly offer a controlled flow of data between the MAC-hs located in the Node-B and the Mac-d located in the RNC in a dynamic manner by taking into account the transmission capabilities of the air interface. This flow control mechanism essentially regulates data flow between the RNC and the Node-B. This flow control algorithm also affects the data flow on the  $U_u$  logical interface. The flow control function needs to be developed to reduce the Layer 2 signaling latency, as well as to reduce missing and retransmitted data that could be caused by HS-DSCH channel congestion. The flow control mechanism is important for maintaining the QoS of uplink and downlink data transmission.
- *Scheduling/priority control.* This function manages HS-DSCH resources between HARQ entities and data flow according to the connection priority. Feedback signaling based on ACK/NACK determines whether transmission or retransmission needs to be initiated.

The MAC-e entity is used to support the HSUPA operation. There is one MAC-e entity in the Node-B for each UE and one E-DCH scheduler function in the Node-B. When the MAC-e is configured by the RRC layer, the MAC-e and the E-DCH scheduler jointly handle the HSUPA functions in the Node-B; they jointly perform the following functions:

- *E-DCH scheduling.* This function manages resources of UEs. The scheduler grants resources to UEs based on their requests. A grant could be absolute or relative as described in the earlier section.
- *E-DCH control.* This entity is responsible for the reception and transmission of scheduling requests.
- *Demultiplexing.* This function is used to demultiplex MAC-e PDUs at the RNC. After demultiplexing the MAC-es PDUs are forwarded to the associated MAC-d flows.
- *HARQ.* A HARQ entity with the MAC-e is capable of supporting multiple stop and wait HARQ processes. Each process is responsible for generating ACKs and NACKs indicating delivery status of each E-DCH PDU.

## 7.4 E-UTRAN Architecture

The Evolved UTRAN (E-UTRAN) framework was developed to support the evolution of 3GPP radio access technology toward a high data rate, lower latency, packet-optimized radio access networking technology [4, 12]. The E-UTRAN standard is developing to support future evolved air interfaces that will support wider transmission bandwidths up to 20 MHz instead of the current 5 MHz, new transmission schemes, and advanced multi-antenna configurations using MIMO (multiple-input, multiple-output) technology. The main targets for the evolution of the radio interface and radio access network architecture include the following:

- Significantly increased peak data rate on both the up- and downlinks. Peak data rates of 100 Mbps on the downlink and 50 Mbps on the uplink is expected in the initial E-UTRAN standard. The plan is that the peak data rate will scale with the bandwidth. It is also expected to offer increased “cell edge bit rate” with the current deployment of Node-Bs.
- Possibility of UTRAN latency (UE to RNC/RNC to UE) of 10 ms or less.
- Support of scalable bandwidth 5, 10, 20, and possibly 15 MHz.
- Support of interworking with 3G systems and other non-3GPP-specified systems such as IEEE802.11 WLAN and IEEE802.16/WiMAX.
- Efficient support of various types of standard and advanced services in the PS domain. New services such as VoIP are contemplated in the near future.
- Support of lower power consumption of user terminals by introducing discontinuous uplink transmission [3, 13].

The E-UTRAN architecture is similar to the UTRAN, with a reduced number of network elements. The overall architecture of E-UTRAN is shown in Figure 7.7. The eNB (E-UTRAN Node-B) replaces Node-B and is connected

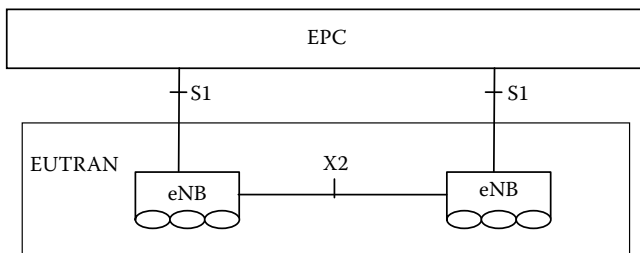


**Figure 7.7** Evolved UTRAN architecture (3GPP, TS36.401, R7, Evolved Universal Terrestrial Radio Access Network (E-UTRAN); Architecture Description, v.8.5.0, Fig. 6.1-1, 10, 2009. With permission from ETSI.)

via the S1 interface to the evolved packet core (EPC) network. Two logical interfaces, S1 and X2, are based on the IP protocols to efficiently support packet-switched traffic. The S1 logical interface replaces the two-hop  $I_{ub}/I_u$  links of the UTRAN. This architecture also eliminates the need for the RNC. An eNB can support FDD (frequency division duplex), TDD (time division duplex), or dual-mode operation. The E-UTRAN architecture is based on an LTE flat network structure where eNB directly communicates with the enhanced core network without the need for the RNC. The eNB will host the following functions:

- *Radio resource management*: radio bearer control, radio admission control, connection mobility control, dynamic resource allocation/scheduling.
- *Mobility management entity*: distribution of paging messages to the eNBs.
- *User plane entity*: IP header compression and encryption of user data streams, termination of U-plane (user plane) packets for paging tasks, switching of U-plane to support UE mobility.

## 7.5 UTRAN Design: $I_{ub}$ Link Resource Management Algorithms

This section presents UTRAN/ $I_{ub}$  specific link resource management algorithms. The  $I_{ub}$  link allocation and its resource management algorithms located in the Node B and the RNC. The resource management algorithms significantly influence the traffic QoS on the  $U_u$  interface. Also, the  $I_{ub}$  link design influences UTRAN resource requirements and the capital cost of system development [14, 15]. In this section, we review the  $I_{ub}$  flow control techniques and analyze the effect of the flow control algorithm on service QoS and UTRAN resource requirements. The UTRAN architecture discussed in the previous section shows that proper dimensioning of the HSDPA RAN is becoming important due to the increasing data rate of the HSDPA air interface and the introduction of more dynamic/bursty traffic sources. The  $I_{ub}$  link is an expensive RAN resource, particularly from the operator's point of view [14]. Some early work by Toskala et al. [16] has shown that with increasing radio link utilization, there is a considerable reduction in the  $I_{ub}$  link utilization. Their work showed that at least 20% over-dimensioning of the  $I_{ub}$  link is necessary to achieve 95% of the maximum available HSDPA air interface capacity. With the increasing HSDPA data rate, this 20% over-dimensioning factor will significantly increase the operational cost of the UTRAN. The over-dimensioning factor could vary with different traffic types and user QoS requirements. To avoid the over dimensioning of the

$I_{ub}$  link, we introduce a joint resource management algorithm that allocates the  $I_{ub}$  link capacity based on the air interface throughput of each HSDPA connection.

As discussed, the HSDPA architecture uses a distributed RAN architecture that requires a flow control algorithm between the RNC and the Node B. Node-B controls the traffic flow on the  $I_{ub}$  link. The RNC sends the buffer space request to the Node-B using the HS-DSCH Capacity Request frame protocol. The Node-B initially allocates a transmission capacity to the RNC for each UE connection using the HS-DSCH Capacity Allocation frame protocol, as shown in the flow diagram in Figure 7.8 [17]. Node-B sets up the initial credit window size and the MAC-PDU size for the RNC. The RNC can send a request to alter the allocated credit size and the MAC-PDU size. The main objectives of the  $I_{ub}$  flow control algorithms include the following:

- Minimize the end-to-end latency between the RNC and the UE.
- Increase the downlink air interface and the  $I_{ub}$  link throughput.
- Support different types of packet schedulers at the Node-B and maintain increased air interface and RAN efficiencies.
- Minimize the  $I_{ub}$  interface signaling traffic.
- Avoid the Node-B buffer overflow or buffer starvation.

Recently, a number of researchers have studied the impact of the  $I_{ub}$  link resource allocation techniques on HSDPA air interface performance. Work by Legg [18] developed a flow control mechanism known as  **$K \times \text{max bits}$**  to maximize throughput and packet delay. The parameter  **$K$**  is an integer used to control the data flow on the  $I_{ub}$  link. The value of  **$K$**  depends on the  $I_{ub}$  link latency. Simulation results show that the packet delay and signaling load on the  $I_{ub}$  link can be reduced by adjusting the value of  **$K$** . The results also show that the flow control mechanism could reduce packet loss on the  $I_{ub}$  link. Necker and Weber [19] studied a flow control algorithm to analyze HSDPA system performance. The authors discuss the effect of control dead times on the link that arise due to signaling delays. The dead time refers to the time when no resource allocation update is made due to high signaling delay. Because of the dead time, the flow control algorithm may not be able to react to data rate fluctuations on the air interface. Simulation studies showed the influence of resource allocation update delay and control dead time on IP packet delays. They also studied the effect of control dead time on the Node-B buffer performance and resource allocation [19]. Bajzik et al. [20] developed a congestion control mechanism on the  $I_{ub}$  link. Using the back-pressure algorithm, a control signal is sent from the Node-B to the MAC-d layer at the RNC to adjust the  $I_{ub}$  link allowable transmission rate. The allowable transmission rate is adjusted based on a threshold-based the Node-B queue management technique. Results show that the back-pressure mechanism can significantly reduce  $I_{ub}$  link packet delays and

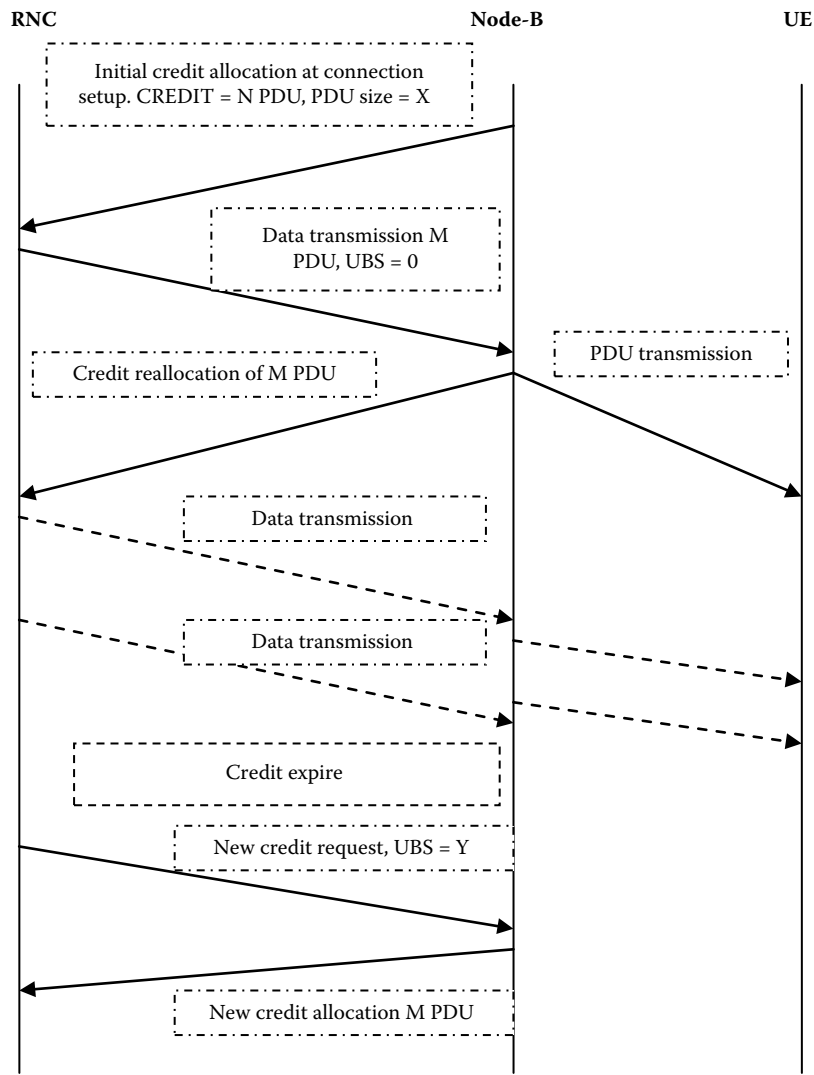
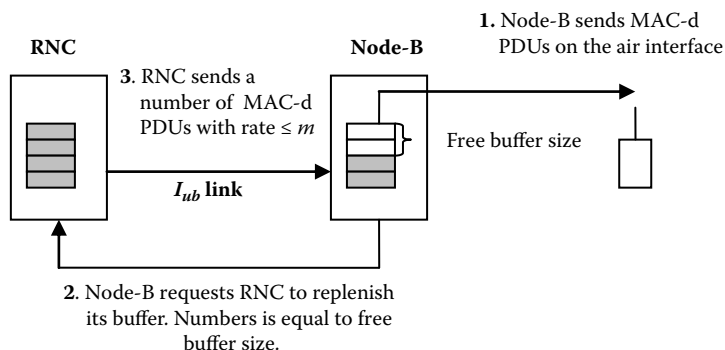


Figure 7.8 RNC credit allocation procedure for HSDPA connections.

retransmission rate. Also, the back-pressure algorithm moderately increases the air interface throughput.

### 7.5.1 Joint $I_{ub}$ Link Flow Control Model

In this section we present a joint  $I_{ub}$  link flow control algorithm. The performance of the algorithm is initially analyzed by using an analytical model. Further performance of the flow control is analyzed using a simulation



**Figure 7.9** Flow control technique employed between Node-B and the RNC. (X. Yan, Khan, J.Y., and B. Jones. *An Adaptive Radio Access Network Resource Management Technique for a HSDPA Network*. 1–5, IEEE, *Proceedings of PIMRC*. 2007. With permission from IEEE.)

model. In the analytical model for each HSDPA downlink connection, we allocate a fixed space in the Node-B buffer, as shown in Figure 7.9. We assume that  $n$  represents the buffer size for each HSDPA connection in the Node-B main buffer, where  $n$  is represented in number of MAC-d PDUs that could be sent over the air interface at the peak transmission rate in every TTI under the best transmission channel conditions. The Node B's main buffer will accommodate all HSDPA connections by allocating buffer space to each connection based on their Qos requirements. We also assume that the  $I_{ub}$  link bandwidth is  $m$  (virtual circuit capacity) for each user connection, where  $m$  is the number of MAC-d PDUs sent in each TTI over the  $I_{ub}$  link. Another assumption used in this model is that the  $I_{ub}$  link creates a separate virtual circuit for each downlink user. After each downlink transmission event on the air interface, Node-B immediately requests the RNC to send more MAC-d PDUs to replenish its buffer. The request size  $R_s$  (in number of PDUs) is equal to the free buffer size. If the requested update size is larger than the  $I_{ub}$  link virtual circuit bandwidth  $m$  (i.e.,  $R_s > m$ ), then only  $m$  MAC-PDUs are delivered to Node-B because attempting to deliver a larger value than the allocated virtual circuit capacity would lead to either  $I_{ub}$  link congestion or a greater delay in refilling the buffer due to the reallocation of  $I_{ub}$  link resources. The value of  $R_s$  can vary between 1 and  $n$ . To avoid low  $I_{ub}$  link utilization, we maintain the relationship that  $m < n$ . Using the above flow control algorithm, the Node-B buffer is used to adjust the HSDPA user throughput on the air interface based on the radio link condition. It is possible that a peak air interface transmission rate may not be sustainable due to the  $I_{ub}$  link and the air interface transmission rate mismatch.

Due to the time-variant nature of radio channels, the transmission data rate of the air interface could be highly variable. We assume that the

transmission rate (expressed in number of MAC-d PDUs per TTI) of an HSDPA connection is distributed between 0 and a maximum number  $n$ . The value of  $n$  depends on the UE category. Let  $r$  represent the air interface rate that the radio channel condition can support in terms of PDUs. Let  $R_i$  represent the probability of air interface transmission rate, where  $i$  represents the number of PDUs transmitted at that rate. After the Node-B transmits PDUs on the air interface, it is assumed that the Node-B immediately requests the RNC to send more packets to replenish its buffer before the next transmission opportunity, as shown in Figure 7.9. Let  $l_n$  be MAC-d PDU numbers in the Node-B buffer measured after the buffer is replenished and waiting for the next transmission opportunity over the air interface in  $n$ th TTI. The buffer length of a user could vary between  $m$  and  $n$ , that is,  $m \leq l_n \leq n$ . We can form a Markov chain using the values of  $l_n$ . Consider the stationary state where all  $\{l_n\}$  have the same probability distribution. Let  $l$  denote the random variable in MAC-d PDU numbers in the Node-B buffer.

$$\text{Let } \pi_i = P\{l = m + i\}, \quad i = 0, \dots, n - m \quad (7.1)$$

The transition matrix  $P$  is shown in the Equation (7.2).

$$\begin{pmatrix} \sum_{i=m}^n R_i & R_{m-1} \dots R_{2m-n+1} & \sum_{i=0}^{2m-n} R_i \\ \sum_{i=m+1}^n R_i & & \sum_{i=0}^{2m-n+1} R_i \\ \vdots & \ddots & \vdots \\ R_n & R_{n-1} \dots R_{n-m-1} & \sum_{i=0}^m R_i \end{pmatrix} (m \leq n \leq 2m) \quad (7.2)$$

In the stationary state, we can write  $\pi = \pi P$ , so

$$\begin{aligned} \pi_0 &= \pi_0 \sum_{i=m}^n R_i + \pi_1 \sum_{i=m+1}^n R_i + \dots + \pi_{n-m} R_n \\ \pi_1 &= \pi_0 R_{m-1} + \pi_1 R_m + \dots + \pi_{n-m} R_{n-1} \\ &\vdots \\ \pi_{n-m-1} &= \pi_0 R_{2m-n+1} + \pi_1 R_{2m-n} + \dots + \pi_{n-m} R_{n-m-1} \\ \pi_{n-m} &= \pi_0 \sum_{i=0}^{2m-n} R_i + \pi_1 \sum_{i=0}^{2m-n+1} R_i + \dots + \pi_{n-m} \sum_{i=0}^m R_i \\ \pi_0 + \pi_1 + \dots + \pi_{n-m} &= 1 \end{aligned} \quad (7.3)$$

We now present a brief analysis to calculate the HSDPA air interface resource utilization. We define the HSDPA air interface resource utilization  $\eta$  as the ratio of the actual number of MAC PDUs (which is limited by the



number of PDUs in the Node-B buffer) that can be transmitted via the air interface to the maximum number of MAC PDUs that can be supported by the air interface in current radio transmission conditions in each TTI, as shown in Equation (7.4). The HSDPA air interface utilization takes into account the radio channel condition, buffer length, and the  $I_{ub}$  link effective bandwidth. For example, on one occasion, if 8 PDUs of an HSDPA connection are waiting in the Node-B buffer but the radio link condition permits transmission of 10 PDUs, then we obtain a  $\eta$  value of 0.8 (8/10). In that case, the downlink has the opportunity to transmit 10 PDUs but the buffer has only 8 PDUs, causing under-utilization of the link.

$$\eta = \frac{\text{Actual\_MAC\_PDU\_Tx}}{\text{Max\_MAC\_PDU\_air}} \quad (7.4)$$

From a statistical point of view, the air interface capacity of a cell will be approximately normally distributed according to the Central Limit Theorem. Because the distribution of air interface rate is discrete, to simplify our analysis, we approximate the HSDPA air interface transmission data rate using the following binomial distribution as shown in Equation (7.5):

$$R_i = \left( \frac{n}{i} \right) p^i (1-p)^{n-i} \quad 0 < i \leq n; \quad 0 < p \leq 1 \quad (7.5)$$

$$\text{mean} = n.p \quad (7.6)$$

$$\text{HSDPA\_throughput\_at\_RLC\_layer} = \frac{n \times p \times \text{RLC\_packet\_size}}{\text{TTI}} \quad (7.7)$$

where  $R_i$  represents the probability of supported air interface transmission rate,  $i$  represents the number of PDUs transmitted at that rate, and  $n$  is equal to the maximum number of MAC-d PDUs that can be sent in every TTI. The value of  $n$  will depend on the UE category. The value of  $p$  depends on cell parameters. We assume a very good and controlled coverage in a small cell, and low user mobility could lead to a higher value of  $p$ , which represents a higher air interface transmission rate for users. The value of  $p$  also depends on the modulation and coding rate of an HSDPA user. The best radio channel condition is represented by the value of  $p = 1$ .

Figure 7.10 shows the probability distribution of air interface transmission rate per TTI for  $p = 0.8$ , and  $n = 10$  for a category 12 UE. The value of  $p = 0.8$  represents an above-average transmission channel condition. The plot shows that for  $p = 0.8$ , there are high probabilities that a UE will transmit 7 to 9 PDUs per TTI more often than other values. However, there is about a 10% probability that the link will transmit either 6 or 10 PDUs. The peak of the plot will shift toward the left for lower values of  $p$ . A similar probability distribution of transmission data rate was reported by an

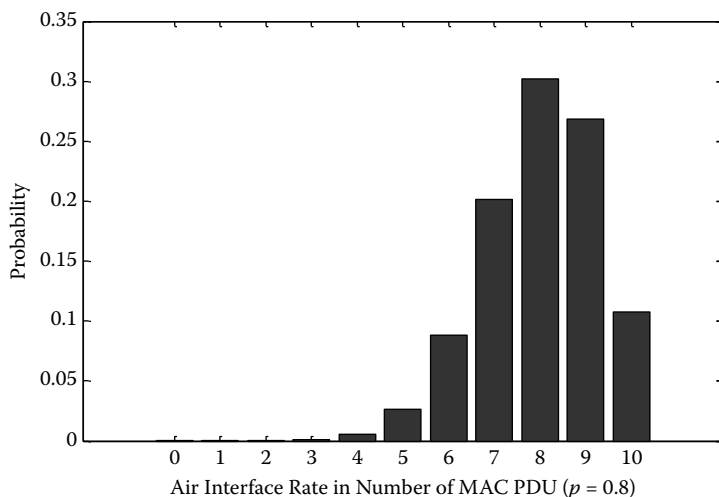


**Figure 7.10** Probability distribution of air interface represented in number of MAC-d PDUs for  $p = 0.8$  and  $n = 10$ . (X. Yan, Khan, J.Y., and B. Jones. *An Adaptive Radio Access Network Resource Management Technique for a HSDPA Network*. 1–5, IEEE, *Proceedings of PIMRC*. 2007. With permission from IEEE.)

Ericsson research group who measured HSDPA network performances in different transmission conditions [21]. The measurement used a test bed of 40 HSDPA sites with category 12 terminals. A measurement was made at the MAC-hs layer with a 10% BLER (block error rate) and a maximum bit rate of 1.5 Mbps. Measurements show that the packet transmission rate varies similarly to our simulation probability distribution with a high probability of transmission between data rates of 0.7 and 1.2 Mbps.

Using the above analytical model described, we can calculate the value of  $\eta$  for a category 12 UE for different air interface conditions and  $I_{ub}$  link capacities. Analysis results are shown in Figure 7.11, where the value of  $\eta$  is plotted against the  $I_{ub}$  link capacity for different air interface throughput and channel conditions. The figure shows that value of  $\eta$  increases with the  $I_{ub}$  link data rate for an RR (Round Robin) packet scheduler. The figure shows that if the  $I_{ub}$  link virtual circuit is allocated the same average capacity as the air interface connection capacity, then we achieve  $\eta = 0.97$ , that is, 97% utilization. If the virtual circuit capacity is lowered, then the value of  $\eta$  decreases. Recall the result of Figure 7.11: for a certain channel condition, the number of MAC PDUs transmitted could vary and, hence, momentary buffer starvation or link under-utilization is possible. The results show that if an HSDPA connection's air interface average throughput is known, and the  $I_{ub}$  link bandwidth is allocated accordingly, then the HSDPA resource utilization factor could reach as high as 97%. In a realistic HSDPA network, the air interface throughput will vary depending on the transmission channel

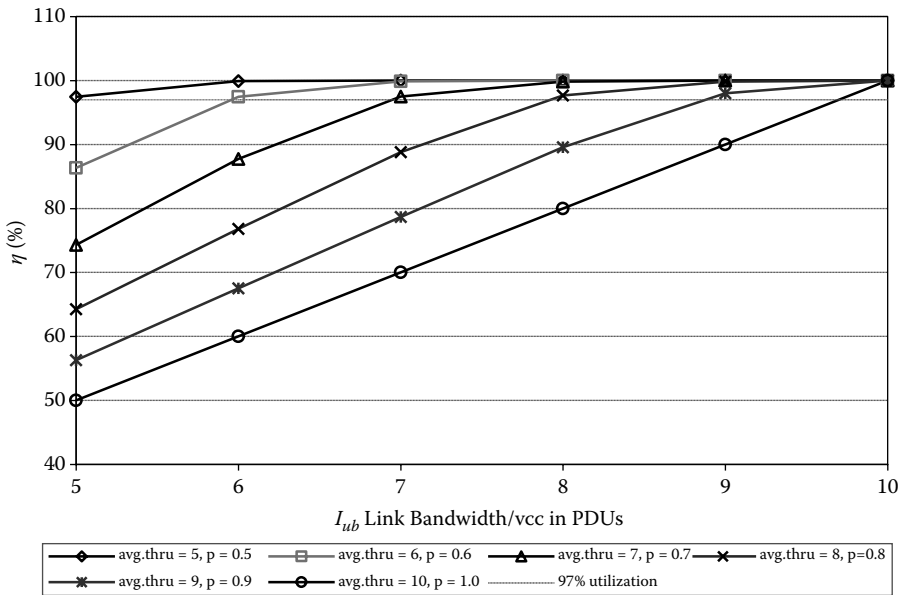


**Figure 7.11** HSDPA resource utilization factor dependency on the  $I_{ub}$  link bandwidth allocation. (X. Yan, Khan, J.Y., and B. Jones. An Adaptive Radio Access Network Resource Management Technique for a HSDPA Network. 1–5, IEEE, *Proceedings of PIMRC*. 2007. With permission from IEEE.)

condition. Hence, a fixed  $I_{ub}$  bandwidth allocation will either reduce the air interface utilization or it will reduce the  $I_{ub}$  link utilization. For example, if the air interface throughput varies between 6 and 8 PDUs, then the  $I_{ub}$  capacity should be matched to obtain higher values of  $\eta$ .

## 7.6 Air Interface and $I_{ub}$ Parameter Interdependencies

This section examines the relationship between the HSDPA air interface and the  $I_{ub}$  link parameters. The results are used to examine the interdependencies of two interface parameters. To examine this interaction we develop a simulation model in addition to the analytical model described in the previous section.

### 7.6.1 Simulation Model

A simulation model was developed to further study the RAN performance for different air interface conditions. The simulator consists of an  $I_{ub}$  interface and a physical link, a traffic generator, an air interface link, and the proposed flow controller as shown in the [Figure 7.12](#). We assume that the core network (CN) can deliver enough packets to the RNC so that a sufficient

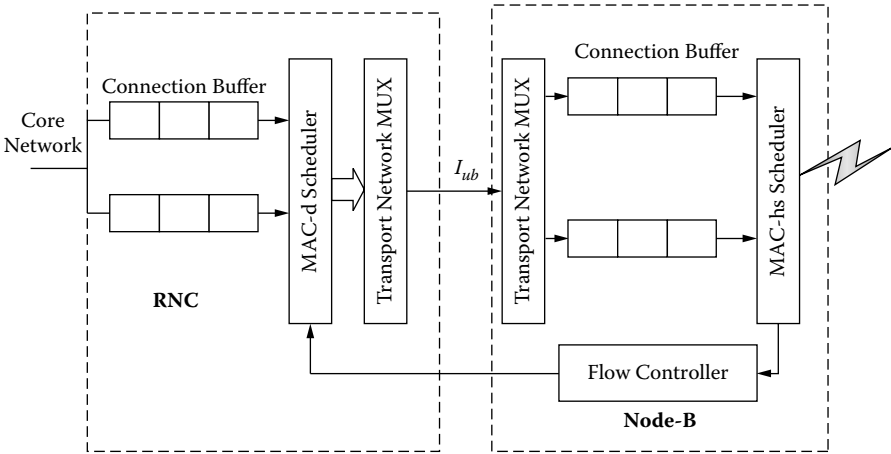


**Figure 7.12** Simulation model block diagram.

number of packets are waiting in the RNC buffer during the active period of a data burst. The flow controller is implemented according to the description given in the “UTRAN Protocol Structure” section. The Node-B allocates each HSDPA connection a transmission bandwidth according to the radio channel condition that is simulated by the binomial distribution as shown in Equation (7.5). The  $I_{ub}$  link is simulated using the AAL2/ATM and UDP/IP transport protocols. The model separately simulates three packet scheduling algorithms: RR, Max C/I (Carrier-to-Interface Ratio), and PF (Proportional Fair). Key simulation parameters are listed in Table 7.2.

### 7.6.2 Performance Analysis

We gathered several simulation and analytical results to study the RAN and air interface parameter interactions. Figure 7.13 shows the relationship between the air interface transmission condition  $p$  and the HSDPA efficiency  $\eta$  for category 5/6 and category 12 UEs using an RR packet scheduler with 15 UEs. The figure shows that the analytical and simulation results are in close agreement. In this simulation, each VC (virtual circuit) capacity on the  $I_{ub}$  link was matched with the average throughput of the respective connections on the downlink. Figure 7.13 shows that the value of  $\eta$  decreases as the transmission capacity of the air interface increases, as represented by the value of  $p$ . The figure also shows that the category 5/6 UE connections perform better than category 12 terminals because of the higher  $I_{ub}$  link data rate. Table 7.2 shows that the category 5/6 terminals were allocated with 18 PDUs for each Virtual Circuit (VC). Category 12 terminals receive 12 PDUs/TTI for each VC. As mentioned earlier, a connection’s buffer in the Node-B is updated by the RNC after every transmission opportunity

**Table 7.2 Key Simulation Parameters**

<i>Simulation Parameter</i>	<i>Value/Features</i>
UE category	5, 6, and 12
Number of UEs	15
$I_{ub}$ link data rate	2.048 Mbps (Cat 5/6), 4.096 Mbps (Cat 12)
$I_{ub}$ link transport protocol	AAL2/ATM and UDP/IP
Maximum buffer allocation for each connection	21 PDU/connection for Cat 5/6 UE, 10 PDU/connection for Cat 12 UE
Virtual circuit capacity	18 PDU/VC for Cat 5/6 UE, 8 PDU/VC for Cat 12 UE
Scheduling algorithm	RR, Max-C/I, PF
Air interface model	Binomial distribution
Traffic model	Web browsing, Pareto distributed based on the UMTS traffic model
PDU size	320 bits

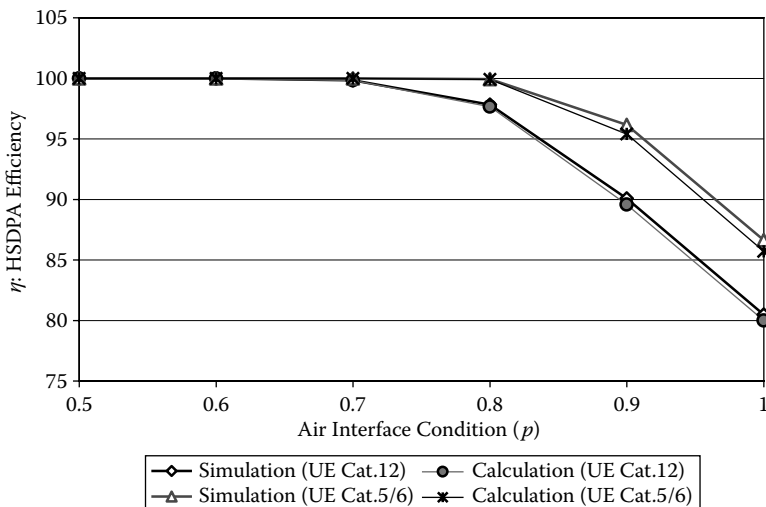


**Figure 7.13** HSDPA efficiency factor variation for different air interface conditions. (X. Yan, J. Y. Khan and B. Jones, Study of Interdependency Between the HSDPA Air Interface and the Radio Access Network, *Proc. of the IEEE 18th PIMRC*, 3–7 September 2007. With permission from IEEE.)

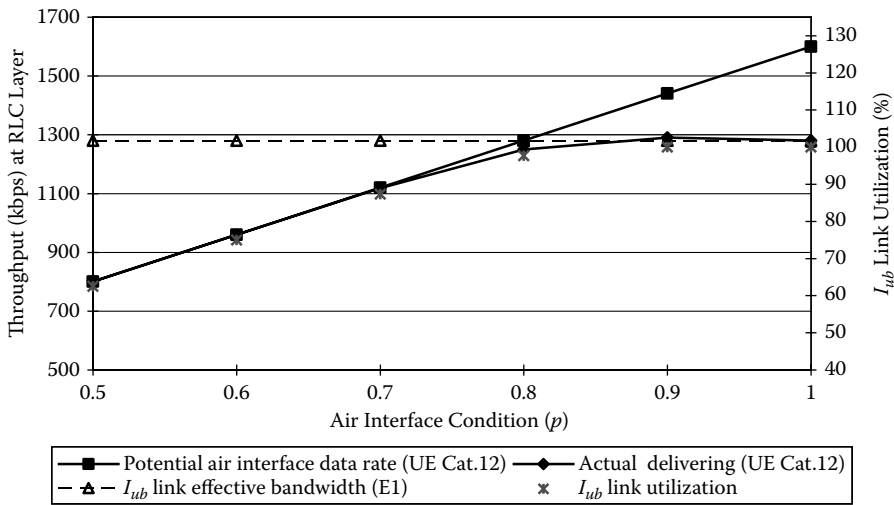


**Figure 7.14** HSDPA throughput measured at the RLC layer for different air interface conditions. (X. Yan, J. Y. Khan and B. Jones, Study of Interdependency Between the HSDPA Air Interface and the Radio Access Network, *Proc. of the IEEE 18th PIMRC*, 3–7 September 2007. With permission from IEEE.)

by the same number of PDUs that were transmitted in the immediate past transmission opportunities. Hence, it is possible that if the air interface transmission rate peaks under a better channel condition, then the  $I_{ub}$  link may not be able to replenish the Node-B buffer with the required number of PDUs, thus resulting in a lower value of  $\eta$ .

Next we observed the relationship between the transmission channel condition and HSDPA throughput measured at the RLC layer. Figure 7.14 shows that it is theoretically possible that the combined air interface throughput can linearly increase with an increasing value of  $p$ . However, the  $I_{ub}$  link latency arises because of the fixed VC capacity allocation and use of fixed-size ATM cell transmissions on the  $I_{ub}$  link. The result shows that the actual throughput of the air interface could reach up to 1.3 Mbps for a 2.048-Mbps link used for the category 12 terminals. Similar results were obtained when a 4.096-Mbps (2xE1) link was used. Results also show that the  $I_{ub}$  link utilization remains low for the lower value of  $p$  due to low throughput of the air interface.

Furthermore, we examined the effect of queue occupancy of each HSDPA connection for different air interface transmission conditions. Figure 7.15 shows the buffer occupancy value for different values of  $p$ . The graph shows that for  $p = 0.7$ , the buffer occupancy level is 10 PDU for 80% of the time where the occupancy level is distributed between the minimum size of 8 PDUs to 10 PDUs for  $p = 0.8$ . For a better channel condition with  $p = 0.9$ ,

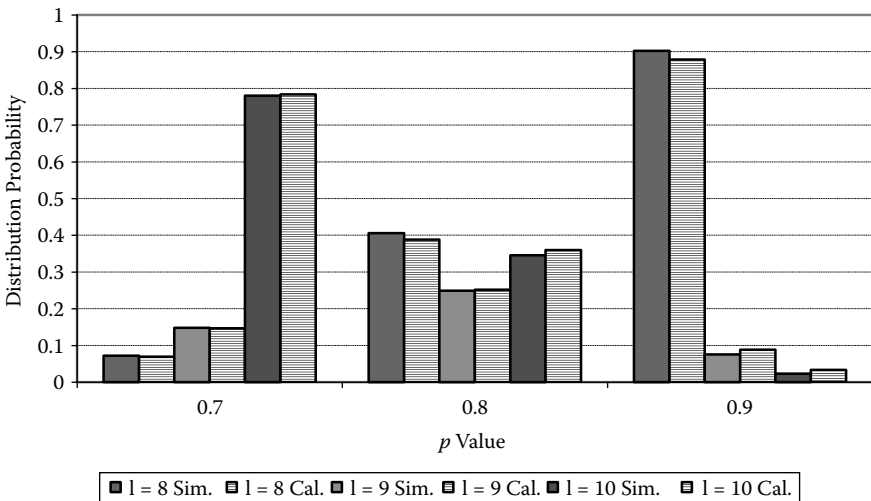


**Figure 7.15** Connection buffer length distribution at Node-B for different air interface conditions. (X. Yan, J. Y. Khan and B. Jones, *Study of Interdependency Between the HSDPA Air Interface and the Radio Access Network*, *Proc. of the IEEE 18th PIMRC*, 3–7 September 2007. With permission from IEEE.)

the buffer occupancy level drops down to 8 PDU due to the higher drain rate by the air interface which is higher than the buffer replenishment rate by the  $I_{ub}$  link. Note that the 8 PDU is the minimum buffer size maintained by each connection.

Next we examined the impact of Node-B scheduling algorithms on the HSDPA throughput. We used a total of 10 category-12 users. In this simulation the value of  $p$  is controlled by a uniform distribution where the value could vary between 0.5 and 1.0. Figure 7.16 shows the cumulative distribution function (CDF) of potential air interface throughput and the actual throughput using three packet schedulers. The Max-C/I fully exploits the available capacity, thus offering the highest potential throughput to some users. The RR scheduler offers a lower potential throughput than Max-C/I but a fairer distribution of resources. The PF scheduler provides a trade-off between the fairness and the capacity. In this case, a modest gain is achieved over the RR scheduler. Throughputs of all these schedulers are affected by the  $I_{ub}$  link resource allocations. It is possible to reduce the latency of the  $I_{ub}$  link by over-allocating virtual circuit capacities but the approach will reduce the link utilization and increase the transmission rate requirements and the cost of a RAN. Figure 7.17 shows the maximum achievable HSDPA efficiency factor for three different packet schedulers. From the RAN resource allocation point of view, we can see that the RR scheduler can operate at a reasonably higher capacity level because of the cyclic air interface transmission schedule, which allows the RAN to supply

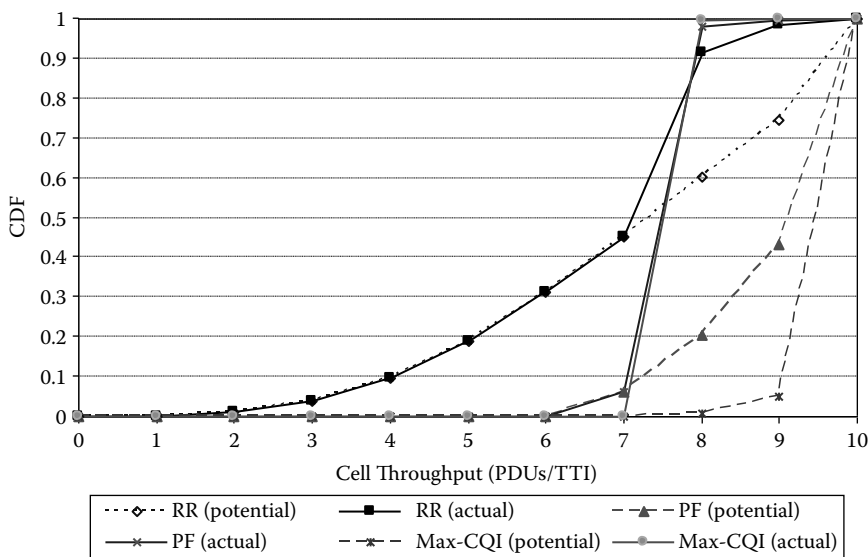


**Figure 7.16** HSDPA cell throughput for every TTI using different packet schedulers. (X. Yan, J. Y. Khan and B. Jones, Study of Interdependency Between the HSDPA Air Interface and the Radio Access Network, *Proc. of the IEEE 18th PIMRC*, 3–7 September 2007. With permission from IEEE.)

a sufficient number of PDUs within the required time. The importance of an adaptive RAN resource allocation technique becomes more important with increasing HSDPA air interface data rates. When the HSDPA network migrates from the current transmission rate of 14.4 Mbps to 40 Mbps in a few years' time, then the network will potentially support 4 to 5 times more users on the downlink. In addition, it is safe to assume that more and more

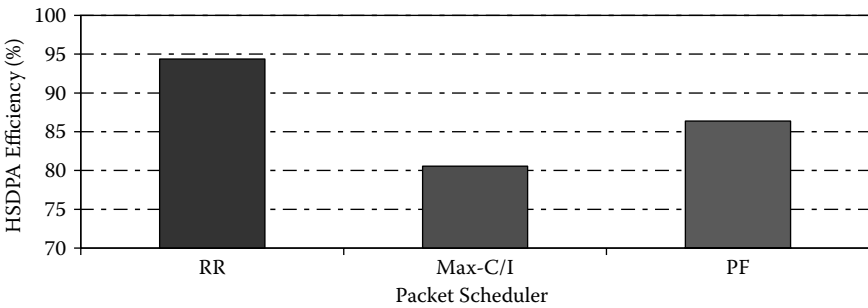


**Figure 7.17** HSDPA efficiency factor for different packet scheduling techniques. (X. Yan, J. Y. Khan and B. Jones, Study of Interdependency Between the HSDPA Air Interface and the Radio Access Network, *Proc. of the IEEE 18th PIMRC*, 3–7 September 2007. With permission from IEEE.)



bursty applications such as video games will be supported on wireless networks in the future, which will increase the ratio of average to peak traffic levels on the RAN. In that case, if an  $I_{ub}$  link is over-dimensioned, then it may be possible that  $I_{ub}$  link utilization will significantly decrease at the same time that the cost of the RAN will increase significantly. Instead of over-dimensioning a RAN, a more prudent approach will be to use adaptive resource allocation techniques on the  $I_{ub}$  link.

In the following section we propose an air interface state information-based  $I_{ub}$  link resource allocation technique.

### 7.6.3 Adaptive $I_{ub}$ Link Management Algorithm

In this section we propose a simple but effective adaptive  $I_{ub}$  link bandwidth allocation technique based on the air interface average throughput. The adaptive resource management algorithm will be located at Node-B, which will measure every HSDPA connection throughput and, using the measured information, will allocate the data rate of the corresponding VCs of the  $I_{ub}$  link by sending the resource allocation packet from the Node-B to the RNC. The feedback-based estimation can offer better utilization of the  $I_{ub}$  link as well as improve the HSDPA efficiency factor.

#### 7.6.3.1 Estimating HSDPA Air Interface Average Throughput

We estimate each HSDPA connection average throughput using a simple averaging equation. Equation (7.8) shows the averaging process. The connection throughput is measured for every burst transmission, and the running average of the air interface throughput is used to allocate on the  $I_{ub}$  link VC bandwidth for that particular connection. The average throughput value is calculated separately for every data burst. When a connection goes to the idle mode, its average throughput value is reset to the default value of  $m$ .

$$\overline{Throughput} = \frac{1}{n} \sum_{i=1}^n x_i \quad (7.8)$$

where  $x_i$  represents the throughput in number of MAC PDUs for the  $i$ th transport opportunity of a connection, and  $n$  represents the transport opportunity numbers.

When  $X_1, X_2, \dots, X_i$  is binomially distributed  $(n, p)$  as in Equation (7.9),

$$\begin{aligned} var(\overline{Throughput}) &= var\left(\frac{1}{N} \sum_{i=1}^N X_i\right) \\ &= \left(\frac{1}{N}\right)^2 \sum_{i=1}^N var(X_i) = \left(\frac{1}{N}\right)^2 Nnp(1-p) = \frac{np(1-p)}{N} \end{aligned} \quad (7.9)$$

### 7.6.3.2 Adaptive $I_{ub}$ Bandwidth Allocation

The scheduler in the Node-B selects an active HSDPA connection to transmit packets on the air interface in every TTI. After each transmission, the Node-B calculates the  $I_{ub}$  connection bandwidth  $\overline{m}$  using throughput value of Equation (7.8). Node-B also calculates the value of  $R_s$  by measuring the buffer length. The Node-B then sends a control message by incorporating the value of the  $I_{ub}$  link's allocated capacity and the request size  $R_s$  for the next transmission. Using the proposed algorithm it is possible to match the air interface throughput rate and the  $I_{ub}$  link throughput. The required aggregate  $I_{ub}$  link bandwidth is calculated using Equation (7.10):

$$Bandwidth = \sum_{i=1}^N s_i \times \overline{m}_i \quad (7.10)$$

where  $s_i$  represents the HSDPA connection  $i$  repetition rate that depends on the scheduling technique used by the Node-B.  $N$  represents the total number of VCs mapped on the  $I_{ub}$  link

Next we compare the HSDPA air interface resource utilization figure for different  $I_{ub}$  link bandwidth allocation techniques. In this simulation we used a total of 15 category-12 UEs. We grouped these 15 UEs into three groups, with each group having 5 UEs. One group was assumed to work in good channel conditions, which support an average of 9 MAC-PDUs per TTI. The second group of 5 UEs was assumed to operate in medium channel conditions with an average of 7 MAC-PDUs per TTI. The third group consisted of 5 UEs operating in poor channel conditions with an average throughput of 5 MAC-PDUs per TTI. In this simulation we used a Round Robin (RR) scheduling technique at the Node-B. In this simulation, first we allocated each VC equal to its downlink peak data rate in terms of number of PDUs. For category-12 UEs, the peak data rate was 10 MAC-d PDU/TTI. After obtaining the simulation results for the fixed virtual capacity, we employed the adaptive virtual circuit capacity allocation algorithm to analyse the performance of both interfaces. Results presented in Figure 7.18 show that the adaptive algorithm reduces the HSDPA air interface utilization only by about 3% but the algorithm reduces the effective  $I_{ub}$  link capacity requirements significantly. Figure 7.19 shows that the  $I_{ub}$  physical link bandwidth requirements and the effective bandwidth utilization for the adaptive allocation and peak rate allocation techniques using the AAL2/ATM and UDP/IP transport protocols. Figure 7.19 also shows that to support the same amount of air interface traffic, the adaptive allocation technique requires about 0.8 Mbps less  $I_{ub}$  link data rate for the AAL2/ATM transport protocol and about 0.7 Mbps less data rate for the UDP/IP protocol. Also, if we compare the link utilization figure, then we see that the adaptive algorithm increases the link utilization by 27%. The proposed algorithm increases

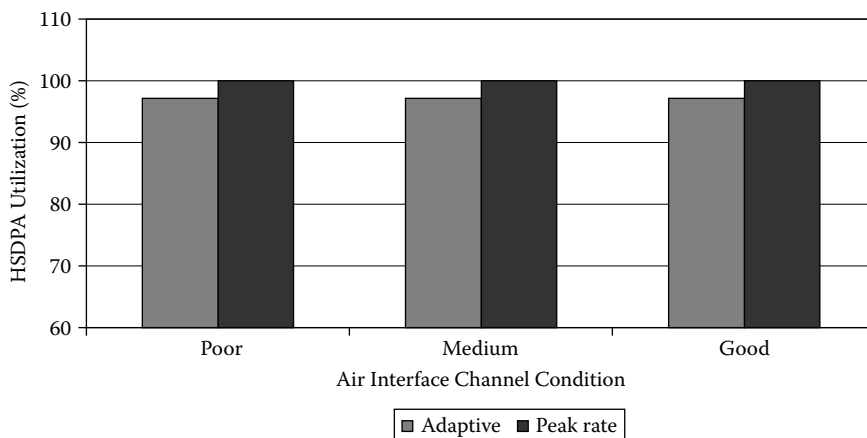


**Figure 7.18** Effect of  $I_{ub}$  link capacity allocation techniques on the HSDPA utilization factor. (X. Yan, Khan, J.Y., and B. Jones. An Adaptive Radio Access Network Resource Management Technique for a HSDPA Network. 1–5, IEEE, *Proceedings of PIMRC*. 2007. With permission from IEEE.)

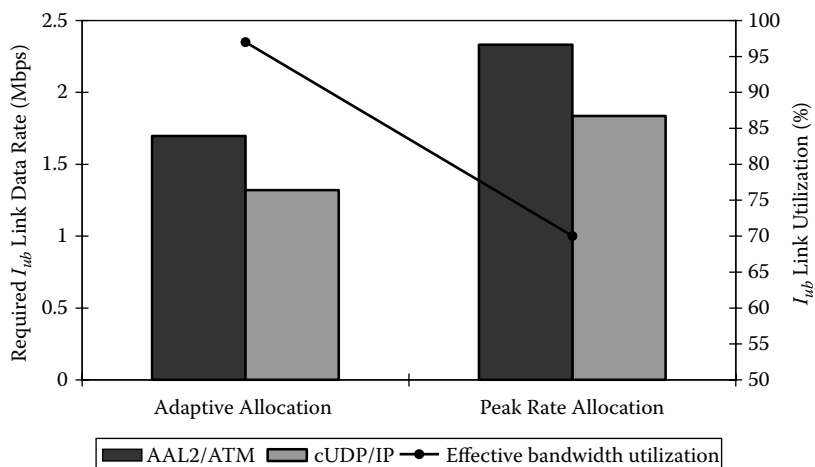


**Figure 7.19**  $I_{ub}$  link transmission data rate requirements for different link capacity allocation techniques. (X. Yan, Khan, J.Y., and B. Jones. An Adaptive Radio Access Network Resource Management Technique for a HSDPA Network. 1–5, IEEE, *Proceedings of PIMRC*. 2007. With permission from IEEE.)

the link utilization, at the same time reducing the  $I_{ub}$  link required transmission rate. Simulation results show that the effect of a variable channel condition can be effectively minimized by implementing appropriate resource allocation techniques presented in this chapter. For a high data rate HSDPA network, the proposed algorithm becomes more appropriate. The proposed algorithm can significantly reduce the operating cost and bandwidth requirements of a RAN.

The proposed joint resource management algorithm can also be extended to HSUPA connections. In case of HSUPA connections, the Node-B to RNC transmission will be supported by the  $I_{ub}$  link. In this case, the  $I_{ub}$  link must be properly dimensioned so that Node-B buffer overflow can be avoided; the overflow could be caused either by the fluctuating radio transmission conditions on the air interface or by  $I_{ub}$  link congestions. Node-B will be able to monitor uplink traffic as well as the uplink transmission condition by measuring the SINR (signal-to-interference-noise ratio) value of each connection. Based on the traffic information and transmission conditions, the Node-B can allocate the appropriate buffer and the  $I_{ub}$  link transmission resources. A recent work by Li et al. [22] investigated the backhaul dimensioning for the HSUPA traffic. They studied an ATM-based  $I_{ub}$  link to support various HSUPA traffic and found that the dimensioning factor of the  $I_{ub}$  link was directly related to the burstiness of the uplink traffic. The dimensioning factor is defined as the ratio of the allocated  $I_{ub}$  link bandwidth to the total HSUPA traffic demands of all UEs in all cells. The work considered the soft handover scenario where Node-B could accept HSUPA traffic from several cells. The authors also concluded that increasing the QoS of HSUPA traffic demands a higher dimensioning factor. Simulation results showed that the dimensioning factor for low to high QoS requirements could vary from 2 to 10. From the operator's point of view, such a dimension factor will be quite expensive; hence, the backhaul network needs to be optimized using adaptive resource allocation algorithms as described for the HSDPA network in this section. The work of Li et al. also showed that congestions on the downlink could affect the throughput and QoS on the uplink. Hence, it is very important that for an HSPA network, joint optimization of resource allocation techniques is necessary to maintain high network throughput and QoS and to reduce the operational cost of a network.

## 7.7 Summary

This chapter introduced the UTRAN and the E-UTRAN architectures for the HSPA standard. Various key functionalities of the UTRAN are presented. The chapter also discussed the E-UTRAN architecture, which will introduce a significant change in the radio access network design. A gradual increase in packet-switched traffic volume in the HSPA network will demand more

flexible IP-based radio access network design. Results presented in this chapter showed that the introduction of IP-based radio access networks will reduce the operational cost of the RAN as well as improve the network resource utilization. Discussions in this chapter showed that it is very important to jointly optimize the resource allocation algorithms in the radio access network to support high data rate connections and QoS for packet-based services on the HSPA air interface. The joint resource management algorithm introduces a new network design paradigm that can be further extended to optimize the UTRAN/E-UTRAN resources.

## References

- [1] 3GPP, TS25.401, R8, UTRAN Overall Description, v.8.2.0, December 2008.
- [2] P. Lescuyer and T. Lucidarme, *Evolved Packet System (EPS): The LTE and SAE Evolution of 3G/UMTS*, Chapter 2, John Wiley & Sons, 2008.
- [3] H. Holma, A. Toskala, K. Ranta-aho, and J. Pirskanen, High speed packet access evolution in 3GPP release 7, *IEEE Commun. Mag.*, 45(12): 29–35, December 2007.
- [4] 3GPP, TR25.913, R8, Requirements of Evolved UTRA (E-UTRA) and Evolved UTRAN (E-UTRAN), v.8.0.0, December 2008.
- [5] 3GPP, TS25.410, R8, UTRAN  $I_u$  Interface: General Aspects and Principles, v.8.0.0, December 2008.
- [6] 3GPP, TS25.420, R8, UTRAN  $I_{ur}$  Interface: General Aspects and Principles, v.8.1.0, December 2008.
- [7] 3GPP, TS25.430, R8, UTRAN  $I_{ub}$  Interface: General Aspects and Principles, v.8.0.0, December 2008.
- [8] 3GPP, TS25.913, R8, High Speed Downlink Packet Access (HSDPA): Overall Description, v.8.4.0, December 2008.
- [9] H. Holma and A. Toskala (Eds.), *WCDMA for UMTS- HSPA Evolution and LTE*, 4th edition, John Wiley & Sons, 2007.
- [10] 3GPP, TS 25.319, R8, Enhanced Uplink Overall Description, v.8.0, March 2009.
- [11] 3GPP, TS25.321, R8, Medium Access Control (MAC) Protocol Specification, v.8.4.0, December 2008.
- [12] 3GPP, TS36.401, R7, Evolved Universal Terrestrial Radio Access Network (E-UTRAN); Architecture Description, v.8.5.0, March 2009.
- [13] 3GPP, TR25.903, R7, Continuous Connectivity for Packet Data Users, v.7.0.0, March 2007.
- [14] Whitepaper, Cost Optimized Transport Evolution—Making the Right Choice, Nokia Corporation, 2006.
- [15] X. Yan, J.Y. Khan, and B. Jones, Study of interdependency between the HSDPA air interface and the radio access network, *Proc. of the IEEE 18th PIMRC*, 3–7 September 2007.
- [16] H. Holma and A. Toskala (Eds.), *HSDPA/HSUPA for UMTS: High Speed Radio Access for Mobile Communications*, John Wiley & Sons, 2006.
- [17] 3GPP, TS25.435, R7, UTRAN  $I_{ub}$  Interface: User Plane Protocols for Common Transport Channel Data Streams, v.7.8.0, March 2008.

- [18] P.J. Legg, Optimised  $I_{ub}$  flow control for UMTS HSDPA, *Proc. of the IEEE VTC 2005*, 4: 2389–2393, 2005.
- [19] N.C. Necker and A. Weber, Impact of Iub Flow Control on HSDPA System Performance, *Proc. IEEE PIMRC 2005*, September 2005, 3: 1703–1707, 2005.
- [20] L. Bajzik, L. Korossy, K. Veijalainen, and C. Vulkan, Cross layer backpressure to improve HSDPA Performance, *Proc. IEEE PIMRC 2006*, September 2006, pp. 1–5.
- [21] J. Derksen, R. Jansen, M. Mayala, and E. Westerberg, HSDPA performance and evolution, *Ericsson Rev.*, 3: 117–120, 2006.
- [22] X. Li, Y. Zaki, T. Weerawardane, A. Timm-Giel, and C. Goerg, HSUPA backhaul bandwidth dimensioning, *Proc. IEEE 19th PIMRC*, 15–18 September 2008.